arXiv:astro-ph/9804007v1 1 Apr 1998

Spiral galaxies with WFPC2: II. The nuclear properties of 40 objects

[1]

C.M. Carollo[2,3,4], M. Stiavelli[4,5,6] & J. Mack[4]

Received _____; accepted _____

[1]Based on observations with the NASA/ESA Hubble Space Telescope, obtained at the Space Telescope Science Institute, which is operated by Association of Universities for Research in Astronomy, Inc. (AURA), under NASA contract NAS5-26555

[2]Hubble Fellow

[3]Johns Hopkins University, 3701 San Martin Dr., Baltimore, MD 21218

[4]Space Telescope Science Institute, 3700 San Martin Dr., Baltimore, MD 21218

[5]On assignment from the Space Science Dept. of the European Space Agency

[6]On leave from the Scuola Normale Superiore, Piazza dei Cavalieri 7, I56126 Pisa, Italy

ABSTRACT

We report the analysis of HST WFPC2 F606W images of 40 spiral galaxies belonging to the sample introduced in Carollo et al. (paper I), where 35 other targets were discussed. We describe the optical morphological properties of the new 40 galaxies, derive the surface brightness profiles for 25 of them, and present the results of photometric decompositions of these profiles into a "bulge" ($R^{1/4}$ or exponential) and a disk component. The analysis of the enlarged sample of 75 galaxies puts on a statistically more solid ground the main results presented in paper I, namely: *I.* In ≈30% of the galaxies, the inner, morphologically-distinct, structures have an irregular appearance. Some of these "irregular bulges" are likely to be currently star forming. *II.* Resolved, central compact sources are detected in about 50% of the galaxies. *III.* The central compact sources in galaxies with nuclear star formation are brighter, for similar sizes, than those in non star forming galaxies. *IV.* The luminosity of the compact sources correlates with the total galactic luminosity.

Furthermore, the analysis of the enlarged sample of 75 objects shows that: *A.* Several of the non-classical inner structures are well fitted by an exponential profile. These "exponential bulges" are fainter than $R^{1/4}$ bulges, for given total galaxy luminosity and (catalog) Hubble type later than Sab. *B.* Irregular/exponential bulges typically host central compact sources. *C.* The central sources are present in all types of disk galaxies, starting with systems as early as S0a. About 60% of Sb to Sc galaxies host a central compact source. Many of the galaxies which host compact sources contain a barred structure. *D.* Galaxies with apparent nuclear star formation, which also host the brightest compact sources, are preferentially the early- and intermediate-type (S0a-Sb) systems. *E.* None of the features depends on environment: isolated and not isolated galaxies show indistinguishable properties.

Independently from the physical nature of the non-classical inner structures, our main conclusion is that a significant fraction of galaxies classified from the ground as

relatively early-type spirals shows a rich variety of central properties, and little or no morphological/photometric evidence for a smooth, $R^{1/4}$-law bulge.

Subject headings: Galaxies: Spirals — Galaxies: Structure — Galaxies: Fundamental Parameters — Galaxies: Nuclei

1. Introduction

This is the second of a series of papers dedicated to the investigation of the (nuclear) properties of spiral galaxies. To this aim, we have started a HST WFPC2 snapshot survey in the F606W filter of a sample of 92 spiral galaxies (complemented by 15 additional early-type galaxies, for a comparison with the literature), 75 of which have already been observed. In the first paper of the series (Carollo et al. 1997a, paper I), we have discussed the optical nuclear morphology (and surface brightness profiles) for 35 of our target galaxies, i.e. the ones observed until the HST servicing mission of February 11, 1997. In this paper, we do the same for the additional 40 targets which have been observed since then, the last of the observations being dated April 15, 1997. Analogously to what done in paper I, we use our measurements to investigate the occurrence of nuclear spiral structure, the properties of the bulge-like components in the inner regions of disk galaxies, the frequency of occurrence of nuclear compact sources, and the relation of the above properties with global galactic properties. Here, the enlarged sample of 75 galaxies allows us to perform a statistical analysis of the frequency of occurrence of the various features as a function of luminosity, Hubble type and environment.

In contrast to the wealth of information on the nuclei of early-type galaxies provided by HST (Crane et al. 1993; Jaffe et al. 1994; Lauer et al. 1995; Carollo et al. 1997b, 1997c; Faber et al. 1997), at the start of our investigation little was known either about the nuclear properties of early-type disk galaxies, or about the relation between the nuclear properties and those of the surrounding galactic structure, e.g., the bulge and/or the inner disk (see the recent review by Wyse, Gilmore & Franx 1997). Phillips et al. (1996) presented WF/PC images for a sample of 20 spirals. That analysis was hampered by the inferior angular resolution of the pre-COSTAR HST; furthermore, the Phillips et al. sample was strongly biased toward late-type galaxies. The exploration of the innermost regions of early-type spirals, i.e. of spheroidals at the low-end side of the luminosity sequence, promises to uncover important aspects regarding the formation of nuclei, and their dependence on environment and dynamical structure. More generally, it may provide a crucial test for bulge – and galaxy – formation scenarios.

This paper is organized as follows. In Section 2 we briefly review the criteria that we adopted to choose the sample of galaxies, and the steps of data reduction performed to derive the surface brightness profiles. In Section 3 we present the morphological properties of the 40 new galaxies, the analytical fits used to derive the luminosities and sizes of their bulges, and the procedures adopted to quantify the luminosities and sizes of their nuclear compact sources. In contrast to paper I, in which the bulge-like components were fitted exclusively with a $R^{1/4}$-law, here we fit the inner bulge-like structures with either a $R^{1/4}$-law or an exponential profile, and report the parameters for the best fitting analytical description. In order to ensure homogeneity in the quantification of the bulge properties, we re-performed the analytical fits also for the galaxies presented in paper I (see Appendix A). In Section 4 we use the enlarged sample of 75 objects to discuss the nuclear versus global properties in early-type spiral galaxies. We summarize our conclusions in Section 5.

2. Sample Description and Data Analysis

A sample of 92 spirals (plus 15 objects chosen among E/S0 and S0/Sa, so as to have a reference sample for comparison with the literature on early-type galaxies) was selected from two catalogs with well-defined diameter limits (the UGC catalog for the northern hemisphere, Nilson 1973, and the ESOLV catalog for the southern hemisphere, Lauberts & Valentijn 1989). The objects were chosen to have: *(i)* Angular diameter larger than 1 arcmin; *(ii)* Regular types *Sa, Sab, Sb,* and *Sbc*; *(iii)* Reliable classification; *(iv)* Redshift < 2500 km/s; *(v)* An inclination angle, estimated from the apparent axial ratio, smaller than 75 degrees. From the resulting sample, we excluded the galaxies already imaged with HST, to optimize the overall investment of HST time. Seventy-five out of the total 107 targets have been observed to date. Of these, 35 were observed from March 1996 up to the February 11th, 1997 HST servicing mission, and constitute the sample for the study presented in paper I. Forty more galaxies were observed from then on, and are presented in this paper. Their apparent B magnitude, distance (derived from the RC3 – de Vaucouleurs et al. 1991 – redshift unless a mean group redshift was available), environment

(for those objects that are not isolated), IRAS flux, full-width HI lines measured at the 20% level, and UGC/ESOLV and RC3 morphological classification, are listed in Table 1. We adopt in the following analysis the Hubble types obtained from the RC3 classification by using the provided conversion table (Table 2 of RC3, which gives $0 = S0a$, $1 = Sa$, $2 = Sab$, ..., $9 = Sm$), since the a posteriori inspection of the `WFPC2` images shows that these give generally a better description of the galaxies than the one given by the UGC/ESOLV types. Consistently with paper I, we here adopt $H_0 = 65$ km/s/Mpc.

For each galaxy we acquired two `WFPC2` F606W exposures of 400 and 200 seconds, respectively, with the galaxy nucleus centered on the PC. Surface photometry was carried out in IRAF by using the `STSDAS` task "ellipse". Isophotal fits were restricted to the PC chip. Details on the isophotal fitting procedure and on the technique used to correct for patchy dust absorption are extensively described in paper I. We were able to derive reliable surface brightness profiles for 25 galaxies. The ubiquitous presence of bright knots in the nuclear regions and strong dust obscuration did not allow us to derive an acceptable isophotal fit for the remaining 15 galaxies.

3. Results

Figure 1 displays the inner $18'' \times 18''$ of the F606W images for the new 40 galaxies. For four of the objects, we show in Figure 2 the unsharp-masking images, which better display their relevant nuclear features. The surface brightness profiles for the 25 galaxies for which we were able to perform the isophotal fits are shown in Figure 3. The substructure visible in most profiles is due, in some cases, to a residual influence of the dust absorption or the star forming regions on the derived profiles; in others, it indicates distinct galactic components identifiable in the images.

3.1. The Inner Structure

The 40 new galaxies show a large variety of nuclear morphologies, similarly to the 35 objects we presented in paper I. Strong knot-like enhancements of luminosity (almost certainly due to star formation) are observed on spiral arms in the nuclear regions of several galaxies. In some galaxies the nuclear star formation occurs in round "rings" or in $m = 1$ spiral arms similar to the star forming rings/arms of nuclear starbursts identified by e.g., Maoz et al. (1996). In several objects spiral structure, as traced by spiral-like dust lanes or the bright knots, reaches down to the innermost accessible scales. In the entire sample of 75 objects, only a fraction ($\approx 40\%$) of the galaxies contains a smooth, classical bulge. The central structure of several other objects has instead an irregular morphology: it is often dwarf-irregular like; in a few cases it is rather elongated, similar to a late-type bar. Occasionally, small "bulge-like" features coexist with nuclear spiral structure. We name these non-classical inner structures "irregular bulges", within the caveats of a morphological classification, which does not allow us to distinguish whether these features are actually "bulges", or rather bars, or even morphologically-distinct parts of the disks. The irregular bulges often host very compact, resolved central sources. In several cases, they are full of bright knots, suggesting that nuclear star formation might also be concentrated in these structures. In $\approx 30\%$ of the sample it is not clear whether a (regular/irregular) bulge is present. According to this rich variety of structure, and consistently with our analysis in paper I, we have grouped the new 40 galaxies in several categories, depending on their nuclear morphology, i.e. we have classified galaxies as hosts of: *(i)* regular bulges (RB); *(ii)* irregular bulges (IB); *(iii)* resolved central compact sources (CS); *(iv)* unresolved, i.e. point-like, nuclear sources (PS); *(v)* nuclear spiral structure (NSS); *(vi)* concentrated nuclear star formation (NSF). The categories are listed by their abbreviated nomenclature in Table 2. Question marks indicate ambiguous identifications due to e.g., strong dust obscuration, star formation, inclination effects. The column "Bar", lists whether a (early- or late-type, nuclear or large-scale) bar is detected ("Y") or not detected ("N") in the `WFPC2` images; a question mark indicates that the presence of a bar is uncertain (e.g., in several galaxies, it is hinted by a square morphology). In a few cases the "bar" identifies the same inner, elongated structure listed as an "irregular bulge". As we stressed in paper I, it is important to note that at the resolution of e.g., the Palomar Observatory Sky Survey, the images

of Figure 1 would have only a few elements, and they would display a much more limited variety of morphologies.

3.2. Analytical Fits to the Bulge-Like Components

In order to estimate quantitatively the physical scale and luminosity of the bulge-like components present in the inner galactic regions, and in contrast with paper I (where we adopted exclusively an $R^{1/4}$-law representation for the inner galactic structure), we fitted the PC surface brightness profiles with *(i)* an $R^{1/4}$-law plus an exponential disk, *(ii)* the sum of two exponential profiles, *(iii)* a single-exponential and *(iv)* a single $R^{1/4}$-law profile. For those galaxies hosting a central compact source, i.e. a distinct nuclear component ($\lesssim 0.3''$) in the surface brightness profile, this was excluded from the fits. The theoretical laws were convolved with the HST Point Spread Function (PSF), derived with Tinytim (Krist 1992) before performing the fits. The use of simulated PSFs obtained by construction at the nominal focus position is not necessarily inferior to the use of archival stars, given that pointlike sources with adequate S/N located near to the nuclei were not available for most of the galaxies, and that focus drifts and breathing modify the PSF profile and affect the flux within a 1 PC pixel radius up to 10% (and within 5 PC pixels up to 5%; Suchkov & Casertano 1997). Our approach of convolving the models rather than deconvolving the data helps to minimize the effects of using a possibly non-perfect PSF.

For each galaxy, the best of the above fits was adopted as descriptive of its surface brightness profile. In Table 2 we report in the column "Fit" the half-light radius R_e in arcseconds and the total magnitude of the inner, i.e. "bulge", components identified by the fits. For the exponential bulges, $R_e \simeq 1.678h$, with h the exponential scale length. The bulge parameters for the galaxies of paper I used in the present analysis are given in Table 3 (see Appendix A). For the two-component fits, the uncertainty on the best fit bulge parameters contains a contribution due to possible "leaking" of flux into/from the disk. We carried out a number of tests in order to assess the robustness of the best fit flux assignment to the bulge. In particular, we performed for each galaxy several bulge-disk decompositions by varying the radial range of the fits, or by fitting the bulge component for a range of predefined disk parameters. The corresponding bulge magnitudes vary by up to 0.3 magnitudes, and the effective radii up to ∼30%; in many cases the uncertainty is smaller than these values. These errors do not affect our conclusions. In Tables 2 and 3, the superscripts

$R^{1/4}$, $R^{1/4}$-*expo*, *expo1* and *expo2* close to the galaxy names identify galaxies whose PC light distribution has been fitted with an $R^{1/4}$-law, an $R^{1/4}$-law plus exponential profile, a single- or a double-exponential profile, respectively. The analytical best fits to the surface brightness profiles are shown in Figure 3 (solid lines for $R^{1/4}$ bulges, and dashed lines for exponential bulges).

The galaxies which are fitted by a single exponential profile have central F606W surface brightness in the range $\approx$ 19-20 mag arcsec^{-2}, i.e., on the bright-end side but compatible with Freeman's law (1970) for disks. In spite of this, in eight out of ten cases, there is morphological evidence that the single-exponential fits describe only the inner structure of systems which likely have two distinct components. The morphology of the inner structure often resembles that of dwarf elliptical galaxies, although somewhat more irregular. A few of these systems have a late-type classification in the RC3; however, similarly to their earlier-type relatives, they clearly display in our `WFPC2` images a morphologically distinct central structure filling most of the PC chip, embedded in a typically quiescent, i.e., non star forming, disk or halo. The latter is clearly visible in the WF chips: it has low surface brightness (typical of the disks described by Bothun et al. 1997), and shows little (or sometimes no) spiral arm structure. The incompleteness of the isophotes, and the low signal-to-noise ratio of these faint outer components in our relatively short exposures, make it impractical to derive for them reliable isophotal fits. Nonetheless, the two-component appearance of these galaxies supports the association of the "dominant" inner structures identified by the single-exponential fits with "exponential bulges". The case of E499G37, a galaxy belonging to the sample of paper I, is ambiguous. This galaxy, similarly to the other eight, hosts a PC-scale dominant single-exponential bulge, which is embedded in a surrounding faint structure. However, it also hosts the most extended central compact source (comparable in size with the smallest exponential bulges; Appendix A; Table 3). For this object, we retain the single-exponential fit to describe its "bulge" and the fit derived in paper I to the inner structure to describe its "compact source". The only galaxy fitted by a single-exponential profile which shows no evidence for a distinct outer component is ESO482G17. For it, we report in Table 3 both the single-exponential best fit parameters describing the entire system, and the bulge parameters derived from a double-exponential fit performed to obtain an upper limit to a

possible inner "bulge" component, for which however there is no morphological evidence.

In contrast with the "dominant, single-exponential bulges", the inner components of the double-exponentials fits are small, faint photometrically-distinct structures embedded in dominant, typically spiral-armed and star forming, disks. In Figure 4 we plot the `WFPC2` mosaiced images for four representative galaxies, hosts of the two classes of "exponential bulges". The figure illustrates the difference between the disk-dominated galaxies fitted by double-exponentials (lower panels: NGC4030, left; NGC6384, right), and the "bulge-dominated" objects fitted by single-exponential profiles (upper panels: ESO508G34, left; NGC4980, right). It is possible that relatively faint "exponential bulges" could be hidden also inside the bright $R^{1/4}$-law bulges. For example, the addition of an exponential component similar to the bulges of e.g., ESO498G5, NGC1325 and NGC2082 would not significantly affect the surface brightness profile of a galaxy like NGC2196, and therefore would not be detected in our photometric study. By contrast, relatively bright exponential bulges such as those of NGC3177, NGC4030 and NGC6384 would affect the inner light profile of NGC2196, which would significantly deviate from an $R^{1/4}$-law.

3.3. The Resolved Central Compact Sources

In order to quantify the luminosities of the compact sources seen in the centers of several galaxies, we used three different approaches. The first two approaches were already used and described paper I, and are here summarized: (1) the contribution from the compact source was fitted with a Gaussian, assuming that the underlying galactic light continuum is well represented by the asymptotic value of the Gaussian wings; and (2) the underlying galactic light was modeled with the task "fit/flat" in `ESO/MIDAS`, this model was subtracted from the image, and the counts in excess were attributed to the central source. In addition to these two sets of measurements, we adopted a third criterion for performing such measurements, namely (3) an iteratively smoothed and compact source masked version of the original frame was subtracted from the latter, and the measurement was performed on the resulting image (containing only the compact source). The

three methods are complementary: they sample the galactic background in different regions, and hence their combined use allows us to estimate the uncertainty in the derived values contributed by the poorly constrained underlying galactic light. We adopted as final the averages of, and as errorbars the mean of the differences between, these three estimates for the luminosity of the central sources. The sizes of the compact sources were taken equal to the FWHM of the best fitting Gaussians of method (1), corrected for the instrumental width of `WFPC2`. The so-derived sizes and luminosities are reported in Table 2 (column "Compact Source"). The third method was also applied to the galaxies presented in paper I, and confirmed the estimates for the compact sources parameters presented there. This ensures the homogeneity of the measurements within the enlarged sample used in our discussion.

In several (often $R^{1/4}$-law) galaxies, e.g., NGC2196, NGC3054, NGC3277, NGC5121, NGC7421, NGC7690, the presence of a compact source is ambiguous, since their central peak in density could be interpreted either as a compact source, or as the inward extrapolation of the outer light profile. For the cases in which the ambiguity is less pronounced and the images show a more convincing evidence for a distinct central structure, e.g., NGC3277, NGC7421 and NGC7690, we list their compact source parameters in Table 2 and append a question mark to the "CS" entry in the last column. For the remaining, less convincing cases, we determined the brightest compact source that could be subtracted from the galaxy without leaving a "hole" in its light distribution. These upper limits are listed in Tables 2 and 3 (column "Compact Source").

3.4. Additional Information on the Individual Galaxies

In addition to the information coded in Table 2, we briefly report below further comments relative to the (nuclear) properties of some of the target galaxies. For the bulge-dominated galaxies whose PC light profile has been described by a single exponential, we report also the visible size of the faint, outer disk-like structure.

ESO 205G7. A small bulge-like component is embedded in the inner bar, and hosts in its very

center a multi-armed spiral (radius $\sim 0.5''$; star forming?). The nucleus of the inner spiral is possibly unresolved. Dust lanes along the bar connect to the central spiral.

ESO 240G12. The outer, faint and irregular component extends to about six exponential scales (i.e., $\approx 35''$) of the fitted single-exponential bulge.

ESO 317G20. Spiral-like dust lane reach close to the very center. Tightly-wound (ring-like) star forming spiral arms are present outside $\sim 4''$ from the center (i.e., inside the fitted R_e). Unclear whether the $R^{1/4}$-law structure is a real bulge or an $R^{1/4}$-law disk (see Kormendy 1993 for an extensive discussion on "dense disks" in the centers of spiral galaxies).

ESO 443G80. Star formation is concentrated in nuclear, i.e. bulge-like, region.

ESO 508G34. The distinct, boxy single-exponential bulge is rounder than the surrounding faint disk. The latter extends to roughly six exponential scales (i.e., $\approx 35''$) of the bulge, and shows hints for weak spiral structure.

ESO 549G18. The fitted exponential bulge is embedded in the present bar-like structure.

ESO 572G22. No obvious spiral arms are detected in the faint, quiescent outer disk, which extends to roughly eight exponential scales (i.e., $\approx 50''$) of the single-exponential bulge. The latter has a very elongated, bar-like morphology. Star formation is concentrated in the nuclear region.

IC 879. Highly elongated, star forming structure embedded in the bar-like component. The faint "spiral arm" may be a tidal feature (NGC 5078 is 2.5 arcmin away).

IC 1555. Irregular, boxy inner morphology. Dust lanes cut the very center.

IC 5256. Highly elongated, star forming structure embedded in the bar-like component.

NGC 406. Clear spiral arm structure extending to about ten exponential scales ($\approx 75''$) of the fitted single-exponential bulge. The bulge might be star forming.

NGC 1325. Spiral-like dust structure down to the nucleus.

NGC 1353. Dust lanes down to the nucleus. The presence of a very small ($\lesssim 1''$) bulge, partly

obscured by dust lanes, cannot be excluded.

NGC 1385. Elongated, star forming structure embedded in the (irregular) bar-like component.

NGC 1640. Spiral-like dust lane down to the nucleus. The bulge-like structure is embedded in an early-type bar, and is fitted by the sum of an $R^{1/4}$-law (inner component, reported in Table 2) and an exponential (outer component, equivalent $R_e \sim 12''$). The two components are morphologically indistinguishable.

NGC 2082. Irregular spiral-like structure reaching close to the center.

NGC 2196. The surface brightness profile is reproduced either by a $R^{1/4}$-law plus exponential profile with parameters as in Table 2, or by a single $R^{1/4}$-law of $\sim 30''$. Visual inspection of the image favours the first interpretation, since spiral arms are present within $30''$.

NGC 3054. Regular bulge embedded in a bar-like structure typical of early-type systems. Dust lanes across nucleus.

NGC 3067. The central bright knot shows substructure; therefore, it was not considered as a "CS" (similarly to what was done for several galaxies of paper I, see Appendix A).

NGC 3277. Spiral-like dust down to the nucleus.

NGC 4030. Tightly-wound (ring-like), flocculent nuclear spiral arms (inside the R_e of the fitted exponential bulge).

NGC 4260. The regular bulge is embedded in an early-type bar. The profile is fitted by a $R^{1/4}$-law with $R_e = 36''$ and $V_{F606W} = 11.2$. This fit clearly includes the bar component, and it has therefore been omitted from our analysis.

NGC 4501. Spiral-like dust lanes down to nucleus.

NGC 4806. The profile is fitted by the sum of two exponentials. The inner exponential has $R_e \simeq 6''$ and $V_{F606W} \simeq 14.2$. The inner component clearly includes part of the disk, and it has been therefore excluded from our analysis. The presence of a very small ($\lesssim 1''$) bulge cannot be

excluded.

NGC 4980. Faint outer disk extending to about six exponential scales (i.e., $\approx 50''$) of the fitted single-exponential bulge. The disk shows hints for very faint spiral structure.

NGC 5121. Nuclear elongated structure (bar?).

NGC 5377. Tightly-wound dust lanes spiraling into nucleus, which is surrounded by a ring-like bright structure. The bulge-like structure is embedded in the bar.

NGC 5448. Strong, irregular dust lanes down to nucleus.

NGC 5985. Nuclear spiral-like dust structure. The $R^{1/4}$-law plus exponential fit describes the bulge and a surrounding bar.

NGC 6384. Dust lane across nucleus. The bulge-like structure is embedded in an early-type bar, and is fitted by the sum of two exponentials: an inner component, reported in Table 2, and an outer component (equivalent $R_e \sim 10''$). The two exponential components are morphologically indistinguishable.

NGC 6810. Central few pixels in the `WFPC2` images are saturated (central surface brightness exceeds 12.2 mag arcs^{-2}).

NGC 7421. Nuclear dust lanes. The profile is fitted by a $R^{1/4}$-law with $R_e = 20.2''$ and $V_{F606W} = 12.6$. This fit clearly includes the bar component, and it has therefore been omitted from our analysis.

4. Discussion

Despite the popularity of the $R^{1/4}$-law for fitting the light profile of the central regions of disk galaxies, growing evidence has accumulated in the years for departures from a $R^{1/4}$ falloff of the central light distribution, often well represented by an exponential profile (e.g., Kormendy & Bruzual 1978; Shaw & Gilmore 1989; Kent, Dame & Fazio 1991; Andredakis & Sanders 1994). In

a recent study based on about 50 spiral galaxies, Andredakis, Peletier & Balcells (1995) have fitted the bulge profiles with the generalized exponential law of Sérsic (1968; $\Sigma(r) = \Sigma_o \exp[-(r/r_o)^{1/n}]$, with $\Sigma(r)$ the surface brightness at the radius r, Σ_o the central surface brightness, r_o a scaling radius and n the exponent variable). These authors found that the exponent n varies with Hubble type: early spirals have essentially $R^{1/4}$ profiles ($n = 4$), and late galaxies have exponential bulges ($n = 1$). Courteau, de Jong & Broeils (1996) also found that most Sb and later-type spirals are best fitted by a double exponential. The `WFPC2` data for our extended sample of 75 galaxies allow us to explore the central properties of disk galaxies on scales one order of magnitude smaller than what it is possible to probe from the ground.

Our findings are consistent and extend the general trend found from the ground. In Figure 5a we show the F606W bulge magnitude derived from our fits, against the total B magnitude of the galaxy. Triangles are the bulges derived from the single-exponential fits, pentagons those from the two-exponential fits, and the three-vertex symbols are bulges of galaxies fitted by a single $R^{1/4}$-law (downward) or an $R^{1/4}$-law plus exponential profile (upward). ESO482G17 is identified in the figure with a filled triangle (its single-exponential fit), and by an asterisk (indicating the upper limit to a possible bulge obtained with the double-exponential fit); for ESO499G37, its single-exponential fit is represented by a small filled triangle, and its large compact source by a small asterisk (see §3.2). The $M(Bulge)$=$M(Galaxy)$ line is plotted (dotted) for reference by assuming $B - F606W = (B - F606W)_{reference} = 0.65$ magnitudes, i.e. a value equal to the estimated average $B - V$ color for the sample. Bulge-dominated ($R^{1/4}$ or exponential) systems lie close to this relation. Dashed lines are plotted to indicate the $M(Bulge)$=$M(Galaxy)$ relation for $B - F606W = (B - F606W)_{reference} \pm 0.5$ magnitudes. The $B - F606W$ color of the galaxies is uncertain within several tens of a magnitude, due to several factors. The catalog B magnitudes and the $B - V$ colors, often converted from the $B - R$ colors, are both uncertain to ≈ 0.2 magnitudes; the F606W filter has a different bandpass from the V filter and, particularly for red objects, the F606W magnitudes can be significantly brighter than V magnitudes ($\approx$ 0.3 magnitudes). Exponential bulges are present in bright ($M_B(galaxy) < -19$ magnitudes), disk-dominated systems, and are typically ≈ 2 magnitudes fainter than their $R^{1/4}$-law relatives for

a given total galactic luminosity. In fainter hosts ($M_B(galaxy) > -19$ magnitudes), exponential bulges become the rule, even in bulge-dominated systems.

In Figure 5b we plot the difference between the bulge magnitude (F606W) and the total B magnitude, versus Hubble type (converted from RC3, see §2). Symbols are as in Figure 5a, although now thin symbols represent isolated galaxies, thick symbols galaxies with one or more neighbours, and large symbols galaxies which host nuclear star formation. ESO482G17 and ESO499G37 are excluded from this plot. It is clear from this figure that some level of misclassification is present (see, e.g., the few Sb-Sc galaxies with high bulge-to-disk ratio). Furthermore, the richness of structure observed in the inner regions of spirals at HST resolution might suggest finer classification schemes that the ones based on ground-based observations. For example, both the faint, small exponential bulges embedded in otherwise normal outer disks (pentagons), and the systems with an inner, dominant exponential component and an outer, quiescent "disk" (triangles), have morphologies dissimilar from those of proto-typical objects of the various Hubble types; catalogs classify the latter from very early- to very late-type spirals, although their appearance is similar. In spite of these caveats, the ground-based classification generally provides an adequate *global* description for most of the galaxies (as also found e.g., by Malkan, Gorjan & Tam 1998 for their sample of active galaxies). A possible approach is therefore to retain such a classification, and increase the allowed range of structural properties within each of its bins. This avoids further subjective arbitrariety in assigning galaxies to a specific bin, and prevents the growth of a large number of morphological subclasses. In this framework, *(i)* "normality" becomes the exception (see also Malkan et al. 1998); *(ii)* there is a dependence of bulge profile on Hubble type (within the limitations given by the fact that for several galaxies the surface brightness profiles could not be obtained): while $R^{1/4}$-law bulges dominate the earlier S0a to Sab classification bins, Sb and later spirals preferentially host exponential bulges (in agreement with the analysis of Courteau et al. 1996). For Sb and later-type galaxies, the centroid-magnitude for the exponential bulges is shifted toward fainter magnitudes, compared to that of $R^{1/4}$ bulges. The results are independent of environment (see mixing of thin/thick symbols). We cannot exclude effects due to our limited statistics and/or selection biases; however, at face-value, exponential

bulges are typically fainter than $R^{1/4}$ bulges, for constant total galactic luminosity and Hubble type Sb or later.

It is remarkable that most exponential structures that we detect in our sample host a resolved central compact source (CS). In Figure 6a we plot the F606W magnitude of the CS against the total galactic B magnitude. Triangles are the CS in single-exponential bulges; pentagons are the CS in double-exponential galaxies; 5-vertex asterisks are CS in galaxies with no isophotal/analytical fit. Three-vertex symbols and 5-vertex stars are the upper limits to the magnitudes of possible CSs in ($R^{1/4}$-law and non-fitted, respectively) galaxies where the presence of these distinct nuclear components is ambiguous. The enlarged sample that we have now available puts on statistically solid grounds the relation between central source and galaxy luminosity suggested in paper I. The brighter the galaxy, the brighter the central source ($M_{F606W,CS} \simeq 24.08 + 1.92 M_{B,galaxy}$ excluding the upper limits; $M_{F606W,CS} \simeq 17.90 + 1.57 M_{B,galaxy}$ when the upper limits are treated as measurements). The CSs in galaxies with nuclear star formation (large symbols) tend to be brighter than those in galaxies with quiescent nuclear appearance (small symbols; a Kolmogorov-Smirnoff test gives a probability of 1.2% that the two samples are drawn from the same distribution, once the upper limits are excluded; the probability is $< 4 \times 10^{-3}$ when the upper limits are included as measurements). Diamonds frame those galaxies which host a large scale or nuclear bar (solid line), or in which the presence of a bar is suggested by e.g. an inner square-like morphology (dotted line). In several cases, the bar is not reported in the catalogs classification. Many hosts of central compact sources contain ($\approx 30\%$) or are likely to contain ($\approx 30\%$) a bar-like structure (based on the optical images).

In Figure 6b we plot the difference between the central compact source magnitude (F606W) and the total galactic B magnitude, versus catalog Hubble type (converted from RC3). Symbols are as in Figure 6a (including large symbols for CSs in galaxies with nuclear star formation, and small symbols for CSs in galaxies with a quiescent nuclear appearance). In this figure, upward symbols represent isolated galaxies, and downward symbols are galaxies with one or more neighbours. Central sources are present in several systems as early as S0a-Sa, and become almost

the default for intermediate type galaxies ($\approx 60\%$ of the Sb to Sc galaxies host a central compact source in their very center; several other S0a to Sb galaxies have a clustering of multiple sources which has not been considered as regular "compact sources" in this study, see §3.4 and Appendix A). Making a clear statement about the frequency of central sources in galaxies of different Hubble type is hampered by possible selection effects, as demonstrated by the several upper limits which populate the region of the diagram relative to faint compact sources in early-type spirals. It is interesting however that the early-type disk systems with nuclear star formation, which often makes the derivation of the bulge light profile impractical, host the brightest central sources (see also Appendix A). Environment seems to have little or no effect on this relationship: isolated and not isolated galaxies are mixed over the entire luminosity range.

The origin of the central compact sources is unclear, and it is possible that in some cases a contribution from an active nucleus is present, especially for the brightest CSs in the early-type spirals. It is in general legitimate to ask whether and how these nuclear sources are related to the formation of the inner structures of disk galaxies. Accurate numerical studies show that infall of dissipative disk material, possibly forming the compact sources, might be enhanced by the presence of a bar, and might even form (exponential) bulge-like structures (e.g., Combes et al. 1990; Hasan, Pfenniger & Norman 1993; Norman, Sellwood & Hasan 1996, and references therein; see also Kormendy 1993 for an extensive discussion on this issue). The high fraction of bars in the hosts of central compact sources and irregular/exponential bulges might be interpreted as offering independent support for such a scenario. Related to this, it is legitimate to question whether the inner irregular/exponential structures, or even some of the $R^{1/4}$-law structures, are real "bulges", i.e., stellar systems dynamically hotter and thicker than the disks, or rather bars or morphologically- and/or photometrically-distinct inner parts of the disks themselves. Kinematic data should help us to distinguish between these scenarios. A further discussion on the physical properties of the non-classical inner structures is presented in Carollo (1998).

5. Conclusions

We have analyzed HST WFPC2 F606W images for 40 spiral galaxies. The targets belong to the sample of 75 objects introduced in Carollo et al. (1997a). We have studied the optical morphological properties of the new 40 galaxies, derived the surface brightness profiles for 25 of them, and fitted the inner bulge components with an $R^{1/4}$ or exponential law.

By using the enlarged sample of 75 galaxies, we have better quantified the main results presented in paper I, namely: *I.* In about 70% of the galaxies there is morphological evidence for the presence of a central component, (morphologically) distinct from the surrounding disk. These "bulges" may have an irregular morphology, and occasionally host nuclear star formation. *II.* Resolved, central compact sources are detected in about 50% of the galaxies. *III.* The central compact sources in (S0a-Sb) galaxies with nuclear star formation are brighter than those hosted by galaxies with a quiescent nuclear appearance. The luminosity of the compact sources positively correlates with the total galactic luminosity at the 99.9% level.

Furthermore, the analysis of the enlarged sample of 75 objects shows that: *I.* Several of the inner, morphologically-distinct structures are well fitted by an exponential profile. The subset of these "exponential bulges" which are embedded in otherwise normal spiral structure appear to be fainter than $R^{1/4}$ bulges, for constant total galactic luminosity and Hubble type. *II.* The central sources are present in several systems as early as S0a-Sa; about 60% of the Sb to Sc galaxies host a central compact source in their very center. *III.* The central star clusters are detected in exponential/irregular bulges, or in bulge-less galaxies. Compact sources embedded in $R^{1/4}$-law bulges would possibly not be detected; however, it seems likely that if born, they would be tidally destroyed by the high nuclear densities of these systems, see Carollo & Stiavelli 1998). *IV.* A large fraction ($\approx 30\%$) of the galaxies which host a central compact source shows a barred structure in the optical images. In several other hosts of compact sources ($\approx 30\%$) the presence of a bar is hinted by e.g., an inner square-like morphology. *V.* Environment seems not to play any role in shaping the nuclear properties of disk galaxies: isolated and not isolated galaxies show the same, and large, variety of properties.

Our main conclusion is that in a significant fraction of galaxies classified from the ground

as relatively early-type spirals, there is little or no morphological/photometrical evidence for a classical, smooth, $R^{1/4}$-law bulge. Our results are fully complementary to, and support, studies that have revealed cold kinematics in dense, $R^{1/4}$-law structures embedded in the Sb and later-type spirals (Kormendy 1993): both weaken the connection between "bulges" and low luminosity ellipticals, and unveil a large complexity in the inner structure of disk galaxies.

We thank Colin Norman, Tim Heckman, and the anonymous referee for helpful comments to an earlier version of this paper. CMC is supported by NASA through the grant HF-1079.01-96a awarded by the Space Telescope Institute, which is operated by the Association of Universities for Research in Astronomy, Inc., for NASA under contract NAS 5-26555. MS and JM acknowledge support from DDRF grant D001.82148. MS acknowledges support from the Italian Space Agency. This research has been partially funded by GRANT GO-06359.01-95A awarded by STScI, and has made use of the NASA/IPAC Extragalactic Database (NED) which is operated by the Jet Propulsion Laboratory, Caltech, under contract with NASA.

Appendix A

In order to homogenize the measurements for the enlarged sample of 75 galaxies, we performed the exponential fits described in §3.2 also for the galaxies presented in paper I. In addition, in contrast with paper I and consistently with §3.2, we excluded from the fits the central compact sources, and repeated the $R^{1/4}$ fits for those galaxies hosting such a component. We adopted as final the best of the two fits ($R^{1/4}$-law or exponential). As a result, several galaxies for which in paper I the analytical fits had identifyed an $R^{1/4}$-law component are now listed instead as hosts of exponential bulges. The new fits have a better χ^2, and generally provide a better description of the morphologically-distinct structures seen in the images.

The bulge and central compact source parameters for the galaxies of paper I used in the present analysis are given in Table 3. For easy referencing, we identify in the Table the source for the analytical fits to the bulges. We have included in the list also those galaxies which have no

good fit or no surface brightness profile, but host a central compact source [whose parameters are taken from paper I, and have been further checked with method (3) of §3.3]. Six galaxies reported as hosts of central compact sources in paper I, namely NGC2397, NGC2964, NGC3885, NGC5879, NGC6000 and IC4390, have been excluded from the present analysis, since in these objects the central source shows substructure and/or might be affected by dust obscuration. Four of the six excluded compact sources are hosted by galaxies with nuclear star formation and morphological types in the range S0a–Sb. They are among the brightest in the sample, and if included, would strengthen the finding that the brightest sources are embedded in the early- to intermediate-type spirals.

REFERENCES

Aalto, S., Booth, R.S, Black J.H., Johansson, L.E.B., 1995, AA, 300, 369

Andredakis, Y.C., Sanders, R.H., 1994, MNRAS, 267, 283

Andredakis, Y.C., Peletier, R.F., Balcells, M., 1995, MNRAS, 275, 874

Arp, H., 1996, AA, 316, 57

Bothun, G., Impey, D., McGaugh, S., 1997, PASP, 109, 745

Bowen, B.V., Blades, J.C., Pettini, M., 1996, ApJ, 464, 141

Burstein D., Heiles C., 1984, ApJS, 54, 33

Braatz, J.A., Wilson, A.S., Henkel, C., 1996, ApJS, 106, 51

Broeils, A.H., van Woerden, H., 1994, AAS, 107, 129

Carilli, C.L., Holdaway, M.A., Ho, P.T.P., de Pree, C.G., 1992, ApJ, 399, 373

Carollo C.M., Stiavelli, M., de Zeeuw, P.T., Mack, J., 1997a, AJ, 114, 2366

Carollo C.M., Franx M., Illingworth G.D., Forbes D., 1997b, ApJ, 481, 711

Carollo C.M., Danziger, I.J., Rich, M., Chen, X., 1997c, ApJ., 491, 545

Carollo C.M., Stiavelli, M., 1998, AJ, in press

Carollo, C.M., 1998, in preparation

Chengalur, J.N., Salpeter, E.E., Terzian, Y., 1993, ApJ, 419, 30

Combes F., Debbasch, F., Friedl, D., Pfenniger, D., 1990, AA, 233, 82

Condon, J.J., Freyer, D.T., Broderick, J.J., 1991, AJ, 101, 362

Coziol, R., Barth, C.S., Demers, S., 1995, MNRAS, 276, 1245

Courteau, S., de Jong, R. S., Broeils, A. H., 1996, ApJ, 457, L73

Crane, P., et al. 1993, AJ, 106, 1371

Davis, D.S., Mushotzky, R.F., Mulchaey, J.S., Worral. D.M., Birkinshaw, W.M., Burstein, D., 1995, ApJ, 444, 582

de Vaucouleurs G., de Vaucouleurs A., Corwin H. G. Jr., Buta R. J., Paturel G., Fouqué P., 1991, Third Reference Catalog of Bright Galaxies, (New York: Springer Verlag) (RC3)

Faber S.M, et al., 1997, AJ, 114, 1771

Freeman, K.C., 1970, ApJ, 160, 811

Garcia A. M., 1993, AAS 100, 47 (LGG)

Geller M. J., Huchra J. P., 1983, ApJS 52, 61 (GH)

Goodrich, R.W., Veilleux, S., Hill, G.J., 1994, ApJ, 442, 521

Harnett, J.I., Loiseau, N., Reuter, H.P., 1990, RMxAA, 21, 245

Hasan H., Pfenniger D., Norman C., 1993, ApJ, 409, 91

Hewitt, A., Burbidge, G., 1991, ApJS, 75, 297

Huchra, J., Burg, R., 1992, ApJ, 393, 90

Ho L. C., Filippenko A. V., Sargent W. L.,, 1995, ApJS, 98, 477

Huchra J. P., Geller M. J., 1982, ApJ 257, 423 (HG)

Jaffe W., Ford H.C., O'Connell R.W., van den Bosch F.C., Ferrarese L., 1994, AJ, 108, 1567

Kent, S.M., Dame, T., Fazio, G., 1991, ApJ, 378, 131

Kirhakos, S.D., Steiner, J. E., 1990, AJ, 99, 1722

Kormendy, J., Bruzual, A. G., 1978, ApJ, 223, L63

Kormendy J., 1993, IAU Symposium 153, Galactic Bulges, eds H.J. Habing, H.B. Dejonghe (Dordrecht: Kluwer), p. 209

Krist, J., 1992, Tinytim v2.1 User's Manual (STScI)

Lauberts A., Valentijn E.A., 1989, The Surface Photometry Catalog of the ESO-Uppsala Galaxies, ESO

Lauer T., et al., 1995, AJ, 110, 2622

Lehnert, M.T., Heckman, T.M., 1995, ApJS, 97, 89

Malkan, M.A., Gorjian, V., Tam, R., 1998, astro-ph#9803123

Maoz D., Filippenko A. V., Ho L. C., Macchetto F.D., Rix H.-W., Schneider D. P., 1996, ApJS, 107, 215

Mouri, H., Kawara, K., Taniguchi, Y., 1993, ApJ, 406, 52

Nilson, P., 1973, Uppsala General Catalog of Galaxies, Uppsala Astron. Obs. Ann., 6

Norman C. A., Sellwood J. A., Hasan H., 1996, ApJ, 462, 114

Phillips A. C., Illingworth G. D., MacKenty J. W., Franx M., 1996, AJ, 111, 1566

Polletta, M., Bassani, L., Malaguti, G., Palumbo, G.G.C., Caroli, E., 1996, ApJS, 106, 399

Rush, B., Malkan, M.A., Fink, H.H., Woges, W., 1996, ApJ, 471, 190

Rush, B., Malkan, M.A., Edelson, R.A., 1996, ApJ, 473, 130

Sérsic, J.-L., 1968, Atlas de Galaxias Australes (Cordoba: Observatorio Astronomico)

Stauffer, J.R., 1982, ApJ, 262, 66

Shaw, M.A., Gilmore, G., 1989, MNRAS, 237, 903

Stocke, J.T., Case, J., Donahue, L., Shull, J.M., Snow, T.P., 1991, ApJ, 374, 72

Suchkov, A., Casertano, S., 1997, WFPC2 Instrument Science Report 97-01

Terlevich, E., Diaz, A.I., Terlevich, R., 1990, MNRAS, 242, 271

VanDyke et al., AJ, 111, 2017

Veron-Cetty, M.-P., Veron, P., 1986, AAS, 66, 335

Vila, M.B., Pedlar, A., Davies, R.D., Hummel, E., Axon, D.J., 1990, MNRAS, 242, 379

Visvanathan, N., Yamada, T., 1996, ApJS, 107, 521

Womble, D.S., 1993, PASP, 105, 1043

Wynn-Williams, G.C., Becklin, E.E., 1993, ApJ, 412, 535

Wyse R. F. G., Gilmore G., Franx M., 1997, ARAA, 35, 637

This manuscript was prepared with the AAS LaTeX macros v3.0.

Fig. 1.— Inner WFPC2 F606W $18'' \times 18''$ of the 40 galaxies. North is up, East is left. These images would only have a few resolution elements in the Palomar Observatory Sky Survey, and the structure we detect would disappear.

Fig. 2.— Unsharp-masking images ($9'' \times 9''$) for NGC 3177, NGC 5121, NGC 5377 and NGC 7690. North is up, East is left.

Fig. 3.— Surface brightness profiles for 25 galaxies of the sample. Shown are the analytical fits to the inner components: solid lines for $R^{1/4}$-law fits, dashed lines for exponential fits. Several galaxies host an exponential bulge.

Fig. 4.— The WFPC2 mosaiced images for four galaxies representative of the two classes of hosts of exponential bulges. The upper panels show two "bulge-dominated" objects fitted by single-exponential profiles (ESO508G34, left; NGC4980, right). The lower panels show two "disk-dominated", double-exponential objects (NGC4030, left; NGC6384, right). The arrows and the orthogonal segments indicate the North and East directions, respectively. They are $\approx 12''$ long.

Fig. 5.— Panel a: The F606W bulge magnitude versus total galactic B magnitude. Triangles represent the bulge-dominated galaxies fitted by a single exponential profile; pentagons are the bulges of disk-dominated galaxies fitted by a double-exponential profile; the three-vertex symbols are bulges of galaxies fitted by a single $R^{1/4}$-law (downward) or an $R^{1/4}$-law plus exponential profile (upward). The single-exponential fit for ESO482G17 is represented by the (large) filled triangle; the large asterisk represent the upper limit obtained with a double-exponential fit to a possible bulge component in this galaxy. The single-exponential fit for ESO499G37 is represented by the small filled triangle; its compact source, the largest of our sample, is represented by the small asterisk. The $M(Bulge)$=$M(Galaxy)$ line is plotted (dashed) by assuming $B-V=0.65$, i.e. the estimated average $B-V$ color for the sample. Dashed lines indicate the $M(Bulge)$=$M(Galaxy)$ relation for $B-F606W=0.65\pm0.5$ magnitudes. Panel b: Bulge minus galaxy "delta-magnitude", i.e. F606W bulge magnitude minus total galactic B magnitude, versus morphological type (obtained converting the RC3 classification, see text). Dashed line and symbols are as in panel a. Thin symbols represent isolated, and thick symbols non-isolated galaxies, respectively; large symbols represent galaxies which host nuclear star fomation. ESO482G17 is excluded from this panel.

Fig. 6.— Panel a: The F606W magnitude of the central compact source versus the total galactic B magnitude. Triangles are the CSs in galaxies with a single-exponential bulge; pentagons are those embedded in double-exponential galaxies; five-vertex asterisks are the CSs in galaxies with no isophotal/analytical fit. Three-vertex symbols and 5-vertex stars are the upper limits to the magnitudes of possible CSs in ($R^{1/4}$-law and non-fitted, respectively) galaxies where the presence of these distinct nuclear components is ambiguous. Large symbols are assigned to galaxies with nuclear star formation; small symbols represent galaxies with a quiescent nuclear appearance. Diamonds frame the symbols relative to galaxies which host (solid line) or are likely to host (dotted line) a bar. Panel b: Central compact source minus galaxy "delta-magnitude", i.e. F606W magnitude of the central compact source minus total galactic B magnitude, versus Hubble type (converted from RC3). Symbols as in panel a.

This figure "carolloII_fig1a.jpg" is available in "jpg" format from:
http://arXiv.org/ps/astro-ph/9804007v1

This figure "carolloII_fig1b.jpg" is available in "jpg" format from:
http://arXiv.org/ps/astro-ph/9804007v1

This figure "carolloII_fig1c.jpg" is available in "jpg" format from:
http://arXiv.org/ps/astro-ph/9804007v1

This figure "carolloII_fig1d.jpg" is available in "jpg" format from:
http://arXiv.org/ps/astro-ph/9804007v1

This figure "carolloII_fig1e.jpg" is available in "jpg" format from:
http://arXiv.org/ps/astro-ph/9804007v1

This figure "carolloII_fig2.jpg" is available in "jpg" format from:

http://arXiv.org/ps/astro-ph/9804007v1

This figure "carolloII_fig3a.gif" is available in "gif" format from:
http://arXiv.org/ps/astro-ph/9804007v1

This figure "carolloII_fig3b.gif" is available in "gif" format from:

http://arXiv.org/ps/astro-ph/9804007v1

This figure "carolloII_fig3c.gif" is available in "gif" format from:
http://arXiv.org/ps/astro-ph/9804007v1

This figure "carolloII_fig4.jpg" is available in "jpg" format from:
http://arXiv.org/ps/astro-ph/9804007v1

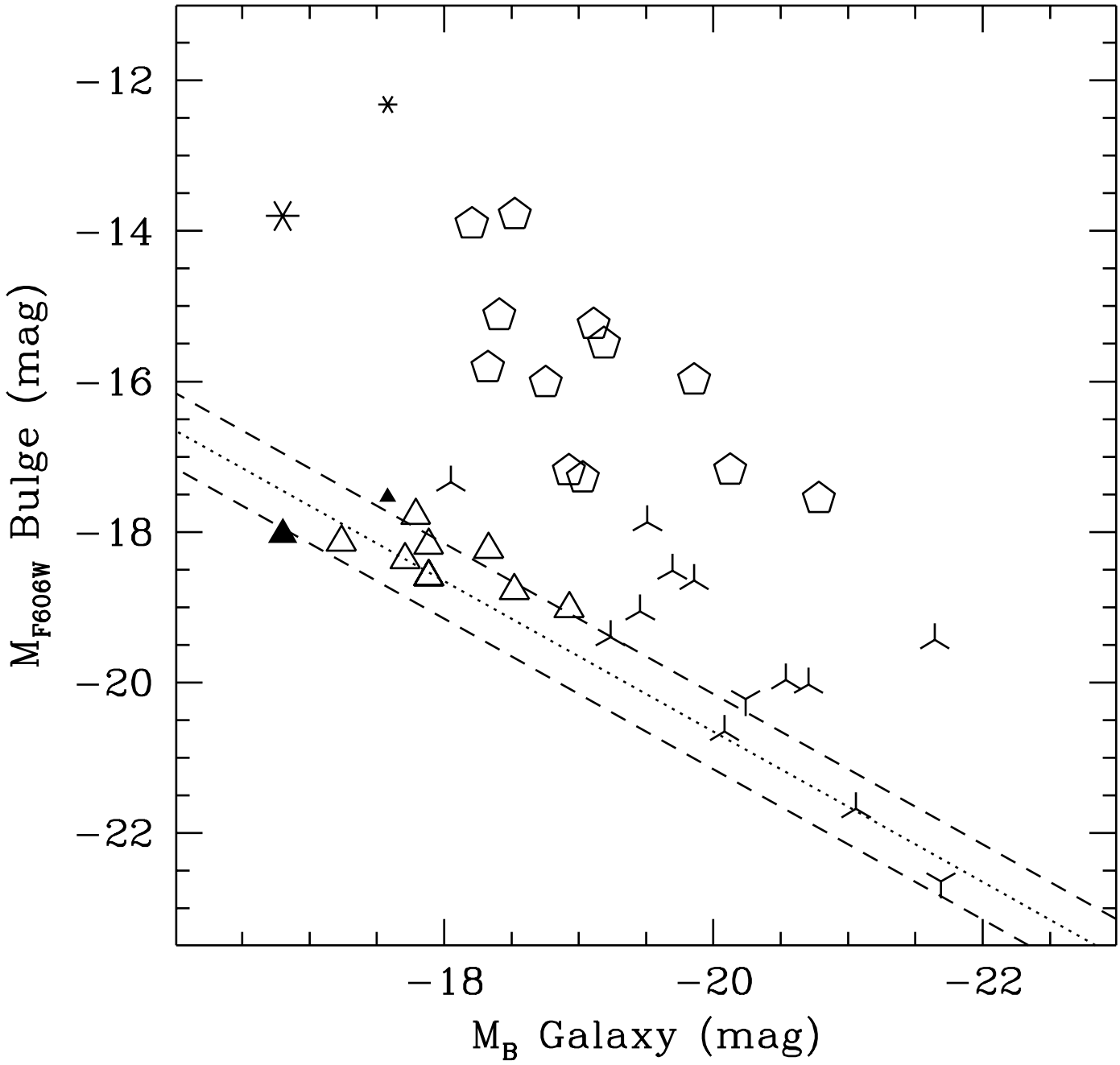
−12
−14
−16
−18
−20
−22
M_{F606W} Bulge (mag)
−18
−20
−22
M_B Galaxy (mag)

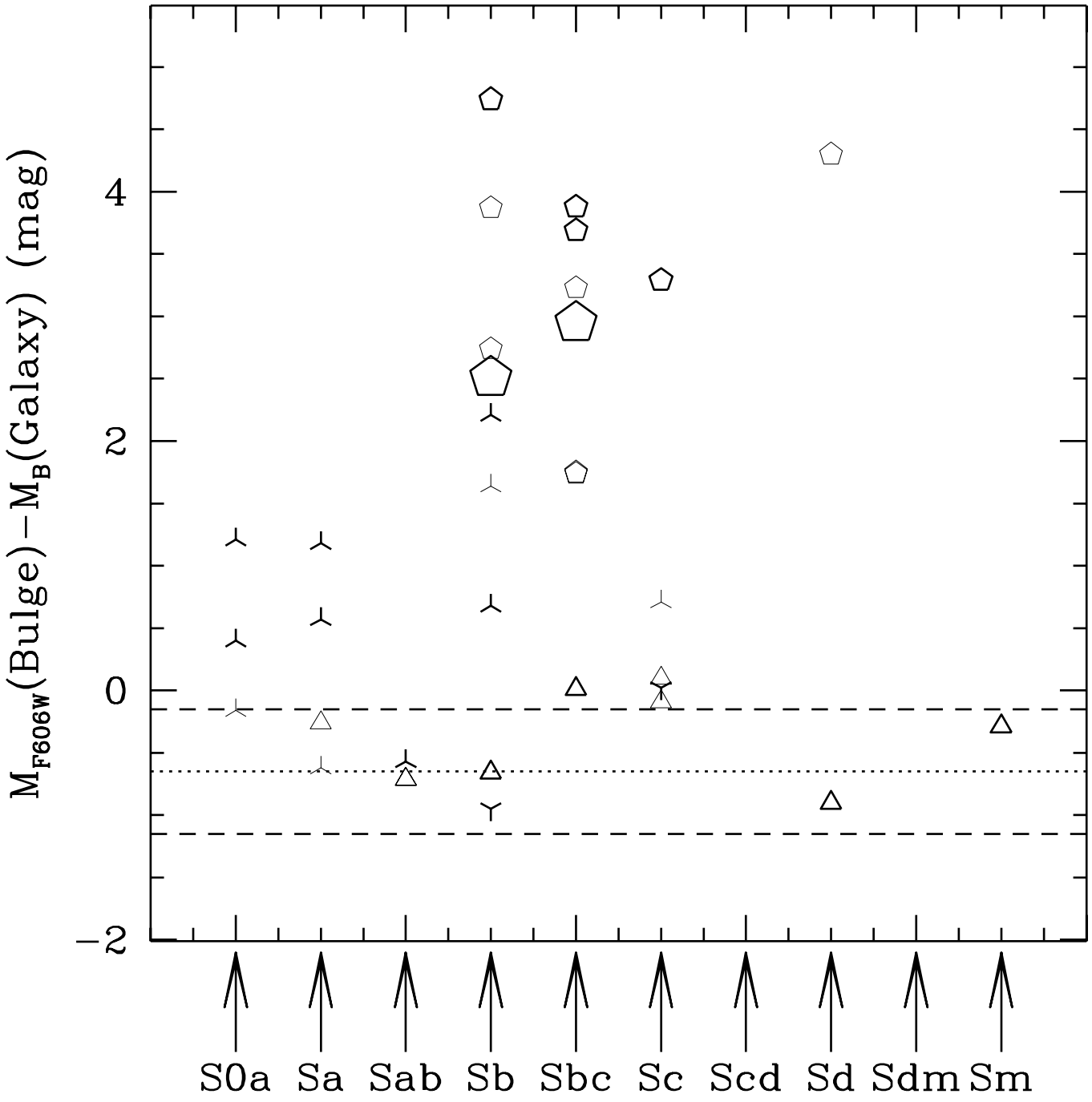
$M_{F606W}(Bulge) - M_B(Galaxy)$ (mag)
4
2
0
−2
S0a
Sa
Sab
Sb
Sbc
Sc
Scd
Sd
Sdm
Sm

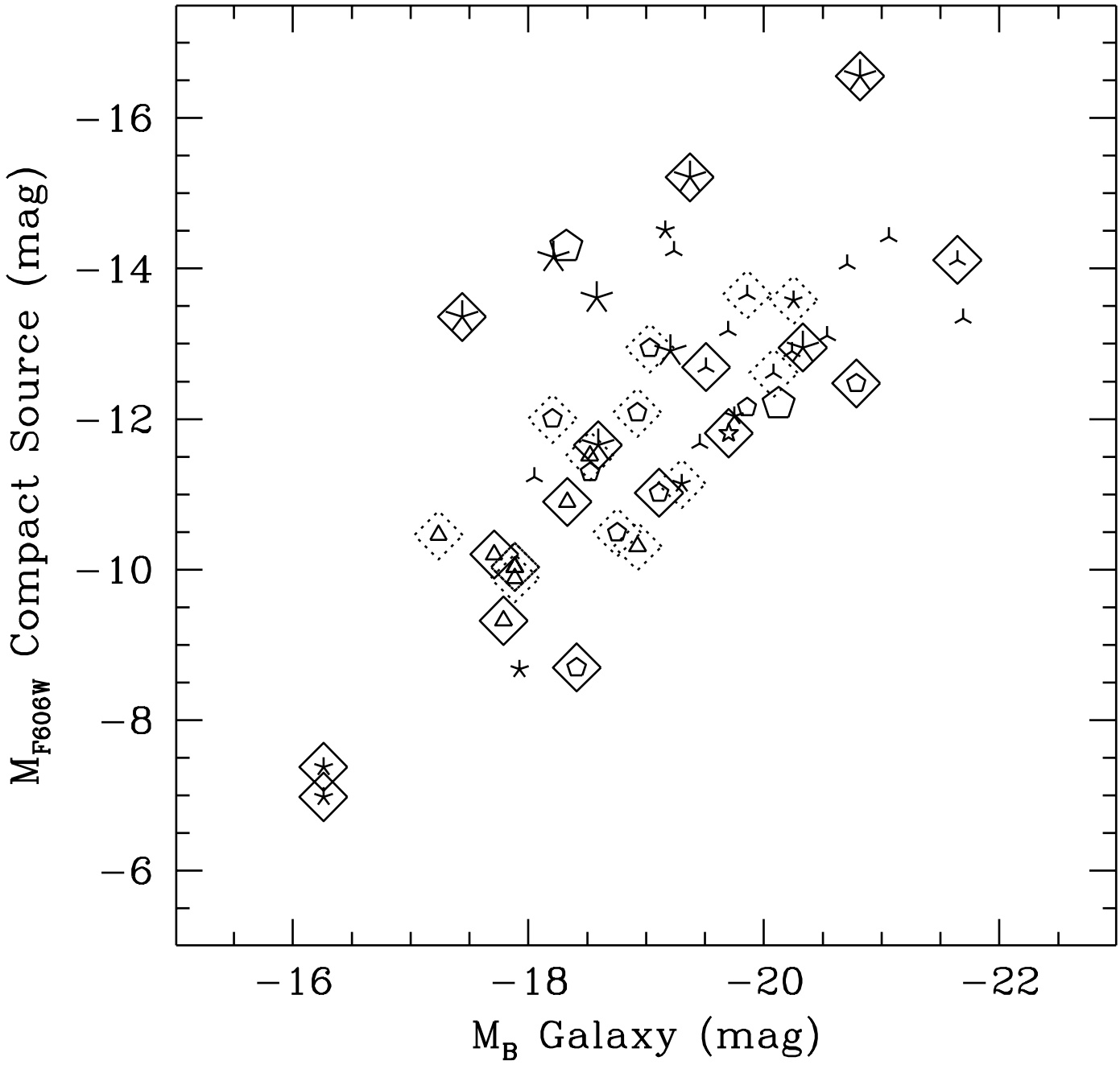
−16
−14
−12
−10
−8
−6
M_{F606W} Compact Source (mag)
−16
−18
−20
−22
M_B Galaxy (mag)

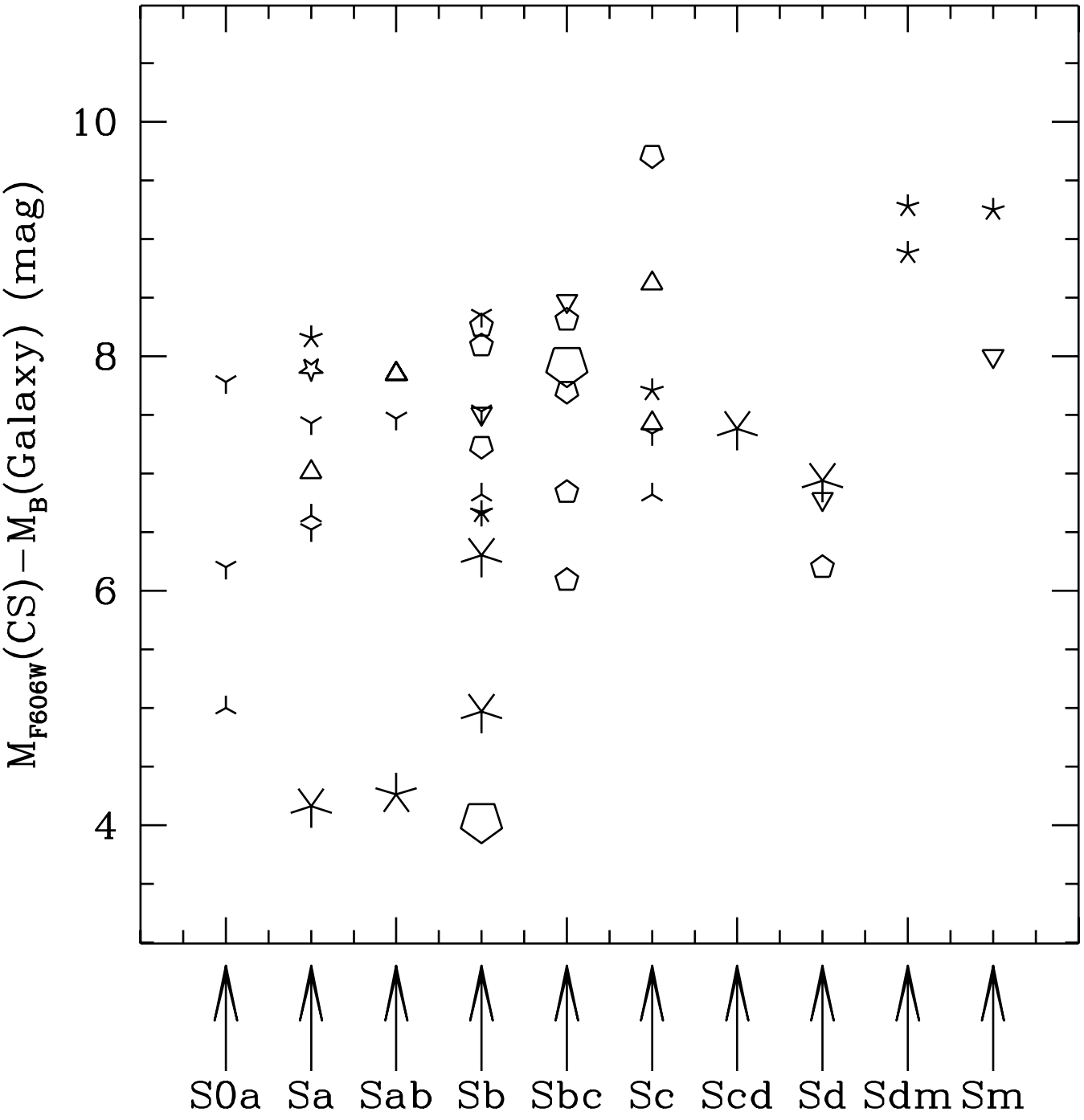
10
8
6
4
$M_{F606W}(CS) - M_B(Galaxy)$ (mag)
S0a
Sa
Sab
Sb
Sbc
Sc
Scd
Sd
Sdm
Sm

Name	D (Mpc)	A_B (mag)	B (mag)	IRAS (mag)	W20 (km s^{-1})	Comments	Type	Environment
ESO 205 G7	31	0.24	15.02*	14.13	-		.SBR3../Sb	
ESO 240 G12	28	0.00	14.35*	13.58	-		.S?..../Sa-b	
ESO 317 G20	38	0.51	12.66*	12.59	-		.SAT5*./Sa	VY [ESO 317 g18]
ESO 443 G80	31	0.29	13.85*	-	-		.SBS9../Sb	LGG331 [3; NGC4965]
ESO 508 G34	29	0.34	14.50*	-	-		.SXS9*./Sb	LGG341/HG31 [8; NGC5061]
ESO 549 G18	24	0.11	13.49*	-	-		.SXT5../Sb	LGG97/HG32-Eridanus [24; NGC1395]
ESO 572 G22	22	0.08	14.92*	-	192		RSB.7P?/Sb	LGG263/HG33 [20; NGC4038]
IC 879	29	0.28	13.73*	-	-		.SBS2P./Sa	LGG341/HG31 [8; NGC5061]
IC 1555	24	0.02	14.37*	-	-		.SAS7../Sb	LGG7 [7; NGC134], CST
IC 5256	15	0.02	14.62*	-	-		.SBS8P./Sb	
NGC 406	23	0.05	13.05	12.51	250		.SAS5*./Sb	
NGC 1325	24	0.04	12.18	12.87	347		.SAS4../Sd	LGG97/HG32-Eridanus [24; NGC1395]
NGC 1353	24	0.03	12.37	11.80	404		.SBT3*./Sb	LGG97/HG32-Eridanus [24; NGC1395]
NGC 1385	24	0.01	11.44	10.03	213	Starburst[a]	.SBS6../Sb	LGG97/HG32-Eridanus [24; NGC1395]
NGC 1640	25	0.00	12.42	12.74	158	Massive SFR[b]	.SBR3../S(r)a	
NGC 2082	19	0.15	12.47	11.83	-		.SBR3../Sb	
NGC 2196	35	0.45	11.37	12.57	392		PSAS1../Sa	
NGC 2339	36	0.61	11.90	9.98	340	Radio Galaxy[c] Lumin.IR Gal[d]	.SXT4../Sb-SBc	
NGC 3045	35	0.12	13.61*	12.47	-		.SAR3?./Sb	
NGC 3054	34	0.28	11.99*	-	403		.SXR3../Sb	LGG185/HG29 [9; NGC3054]
NGC 3067	23	0.07	12.71	10.68	256	Starburst[e] Quasar-GalaxyPair[f]	.SAS2$./Sa-b	
NGC 3177	19	0.07	12.97	10.70	293		.SAT3../Sb	LGG194/GH58,61/HG57 [13; NGC3227]
NGC 3277	21	0.03	12.47	13.26	381		.SAR2../Sa-Sb	LGG197/GH60/HG62 [5; NGC3254]
NGC 3455	19	0.02	-	12.76	215		PSXT3../Sb	LGG219/GH68/HG56 [5; NGC3370]
NGC 4030	20	0.03	-	9.88	347		.SAS4../Sb	LGC264 [4; NGC4030]
NGC 4260	31	0.00	12.70	14.32	471		.SBS1../SBa	LGG278/GH106/HG41-Virgo [8; NGC4261]
NGC 4501	34	0.10	10.26	9.60	532	AGN, LINER, Radio, Seyfert 1,2[g,h,i,j,k]	.SAT3../Sb-Sc	LGG285/GH106/HG41-Virgo [25; NGC4501]
NGC 4806	37	0.35	13.09*	12.44	-		.SBS5?./Sb	
NGC 4980	22	0.34	13.19*	13.42	-		.SXT1P?/Sa	
NGC 5121	19	0.24	11.27	14.03	-		PSAS1../Sa	LGG349 [4; NGC5121]
NGC 5188	36	0.17	12.79	9.82	-	HII[l]	PSXS3P*/Sa-b	
NGC 5377	22	0.00	12.24	12.89	381		RSBS1../SBa	LGG372/GH135/HG72 [7; NGC5448]
NGC 5448	32	0.04	11.89	12.32	417		RSXR1../SBb	LGG372/GH135/HG72 [7; NGC5448]
NGC 5806	20	0.17	12.23	11.80	327		.SXS3../Sb	LGG392/GH150/HG50 [6; NGC5806]
NGC 5985	46	0.02	11.85	12.40	530	AGN[j]	.SXR3../Sb BV [NGC5982]	LGG402/GH158 [4; NGC5985],
NGC 6239	14	0.01	12.93	11.80	231		.SBS3P$/SB	
NGC 6384	26	0.44	10.70	11.62	378	LINER[l]	.SXR4../Sb	
NGC 6810	30	0.18	12.19	9.97	-	Radio Galaxy[k] Sey 2[m], AGN[n] Starburst[o]	.SAS2*/Sb	
NGC 7421	26	0.04	12.52	-	166		.SBT4../Sb-c	LGG466/HG15 [5; IC1459]
NGC 7690	21	0.00	13.00	12.23	266		.SAR3*$/Sb	CST

Table 1: Parameters for the 40 galaxies. Distance D, total blue magnitude B, IRAS magnitudes (mag = -20-2.5 $\log F_{IR}$, where F_{IR} in Wm^{-2} is the weighted average of the flux at 60μ and 100μ), and HI velocity widths at 20% of flux (W20), are from the RC3 catalog (de Vaucouleurs et al 1991). The Galactic Absorption A_B is from Burstein & Heiles (1982, 1984). For the B magnitude, an asterisk indicates Cousins B measurements; values have been corrected for Galactic extinction. Morphological classifications are from the RC3 (left) and UGC or ESOLV (right) catalogs. Information about the galaxy spectrum is taken from: [a] Coziol et al. 1995; Harnett et al. 1990; [b] Van Dyke et al. 1996; [c] Condon et al. 1991; Vila et al. 1990; [d] Wynn-Williams & Becklin 1993; [e] Lehnert et al. 1995; [f] Arp 1996; Womble 1993; Carilli & Gorkom 1992; Stocke et al. 1991; [g] Rush et al. 1996; Veron-Cetty & Veron 1986; Stauffer 1982; [h] Guiricin et al. 1994; Huchra & Burg 1992; [i] Ho et al. 1995; [j] Braatz et al. 1996; [k] Condon et al. 1991; [l] Terlevich et al. 1990; [m] Polletta et al. 1996; Rush et al. 1996; Goodrich et al. 1994; Hewitt et al. 1991; [n] Kirhakos & Steiner 1990; [o] Mouri et al. 1993; Aalto et al. 1995. The environment is given for those objects which are not isolated. The references are: Garcia 1993 (LGG); Huchra & Geller 1982 (HG); Geller & Huchra 1983 (GH); Visvanathan & Yamada 1996 (VY); Chengalur et al. 1993 (CST); and Broeils & Van Woerden 1994 (BV). The number of members and the brightest member of the group/cluster (or the other pair member for a pair [VY,CST,BV]) are given in square brackets.

Name	Bulge	Compact Source† ($''$, mag)	Fit‡ (mag, $''$)	Bar	Comments
ESO 205 G7	IB	0.05 ± 0.02, 19.1 ± 0.2	NGF	Y	NSF; PS?
ESO 240 G12$^{\circ,expo1}$	IB	< 0.03, 22.2 ± 0.1	13.64, 9.67	?	
ESO 317 G20$^{\circ,R^{1/4}}$	RB	> 20	12.68, 11.83	N	
ESO 443 G80°	IB		NSBP	?	
ESO 508 G34^{expo1}	IB	0.06 ± 0.01, 22.5 ± 0.2 0.19 ± 0.01, 21.3 ± 0.1	14.21, 9.97	?	The CS is not on isophotal center; second CS: offset by 1.6"
ESO 549 G18^{expo2}	RB	0.09 ± 0.01, 23.2 ± 0.1	16.78, 3.75	Y	
ESO 572 G22$^{\circ,expo1}$	IB	0.06 ± 0.02, 21.7 ± 0.1	14.02, 10.41	?	
IC 879°	IB		NSBP	Y	NSF
IC 1555$^{\circ,SFRNS}$	IB		NSBP	N	
IC 5256°	IB	< 0.034, 23.5 ± 0.2 < 0.028, 23.9 ± 0.2	NSBP	Y	PS?; second PS: offset by 0.58"
NGC 406$^{\circ,expo1}$	IB	0.04 ± 0.01, 21.5 ± 0.3	12.79, 13.07	?	
NGC 1325^{expo2}	RB	0.09 ± 0.01, 20.0 ± 0.1	16.18, 1.85	N	
NGC 1353*	No?		NSBP	N	NSS
NGC 1385°	IB	0.04 ± 0.01, 19.0 ± 0.1	NSBP	Y	NSF; No well-defined center
NGC 1640$^{R^{1/4}+expo}$	RB	> 19.3	14.12, 2.47	Y	
NGC 2082*,$^{\circ,expo2}$	IB	0.08 ± 0.01, 20.9 ± 0.3	15.38, 3.70	?	
NGC 2196$^{R^{1/4}+expo}$	RB	> 18.3	11.04, 22.94	N	
NGC 2339*,^{SFRNS}	IB		NSBP	Y	NSF; NSS
NGC 3045*,^{expo2}	IB	0.08 ± 0.01, 21.7 ± 0.1	17.48, 0.86	Y	NSS
NGC 3054$^{R^{1/4}+expo}$	RB	> 18.6	12.63, 9.31	Y	
NGC 3067*,$^{\circ}$	IB		NSBP	-	NSF?; No well defined center
NGC 3177$^{\circ,SFRNS,expo2}$	RB	0.09 ± 0.01, 17.1 ± 0.1	15.58, 0.42	N	NSS; NSF
NGC 3277	RB	0.17 ± 0.01,17.2 ± 0.3	NGF	N	CS?
NGC 3455$^{\circ,expo2}$	IB	0.07 ± 0.01, 20.1 ± 0.2	17.61, 1.53	N	NSS
NGC 4030^{expo2}	IB	0.09 ± 0.02, 19.3 ± 0.2	14.33, 2.0	N	NSS
NGC 4260	RB	> 20.5	NGF	Y	
NGC 4501*	?		NSBP	-	
NGC 4806°	IB	0.07 ± 0.01, 20.8 ± 0.2	NGF	N	NSS
NGC 4980$^{\circ,expo1}$	IB	0.07 ± 0.02, 20.2 ± 0.2	12.93, 12.81	?	
NGC 5121$^{R^{1/4}+expo}$	RB	> 18.7	11.84, 7.10	N	
NGC 5188*,$^{\circ}$	No?	0.08 ± 0.01, 19.2 ± 0.3 0.12 ± 0.04, 19.4 ± 0.3	NSBP	?	NSF; the CS is a sum of multi-components second CS offset by 0.38"
NGC 5377*	RB	0.26 ± 0.01, 16.5 ± 0.2	NSBP	Y	NSF? CS?
NGC 5448*	RB		NSBP	?	NSF?
NGC 5806$^{\circ,SFRNS}$	IB?	0.15 ± 0.02, 18.6 ± 0.5	NSBP	-	NSF; NSS; CS?
NGC 5985$^{R^{1/4}+expo}$	RB	> 19.2	13.88, 8.0	Y	NSS?
NGC 6239°	?		NSBP	?	NSF
NGC 6384^{expo2}	RB	0.10 ± 0.02, 19.6 ± 0.6	14.52, 1.95	Y	
NGC 6810*	?		NSBP	N	NSF
NGC 7421	RB	0.10 ± 0.03, 19.0 ± 0.5	NGF	Y	CS?
NGC 7690	No?	0.13 ± 0.01, 18.0 ± 0.7	NGF	N	NSF?; NSS; CS?

Table 2: Summary of nuclear properties. All galaxies have nuclear dust. * indicates a nuclear morphology heavily influenced by patchy dust obscuration. $^{\circ}$ indicates that the inner galactic region contains several bright sources (likely star forming regions). ^{SFRNS} indicates a morphology similar to the star forming rings/arms in nuclear starbursts. † The column gives the FWHM (in $''$) and the apparent F606W magnitudes, obtained directly from the images, for the resolved central compact sources (or point-like sources). ‡ The column lists the the total apparent magnitude in F606W and the half-light radius R_e (in $''$) of the bulge-like components identified by the analytical fits to the surface brightness profiles. Close to the galaxy name, the superscript $R^{1/4}$, $R^{1/4}$-*expo*, *expo1* or *expo2* identifies galaxies whose PC surface brightness distribution has been fitted with an $R^{1/4}$-law, an $R^{1/4}$-law plus exponential profile, a single- or double-exponential profile, respectively. Cases without a good fit are identified by "NGF"; the galaxies for which no surface brightness profile could be derived are identified by "NSBP". In the column "Bulge" the symbols "RB", "IB", and "No" indicate respectively the presence of a regular or irregular bulge-like feature, or no obvious photometric evidence for a bulge-like feature. The column "Bar", lists whether a (early- or late-type, nuclear or large-scale) bar is detected ("Y") or undetected ("N") in the `WFPC2` images; a question mark indicates that the presence of a bar is uncertain. In the last column, "CS" indicates a resolved central compact source, "PS" an unresolved, i.e. point-like, nuclear source, "NSS" spiral structure reaching the nucleus, and "NSF" concentrated nuclear star formation. Question marks indicate doubtful identifications. All magnitudes are corrected for Galactic extinction.

Name	Compact Source† ($''$, mag)	Fit‡ (mag, $''$)	Bar	Reference
ESO 482 G17$^{\circ,expo1}$	0.15 ± 0.14, 20.6±0.3	13.87, 16.79	?	this work
ESO 482 G17^{expo2}		18.10, 4.17		this work (upper limit)
ESO 498 G5$^{\circ,\odot,expo2}$	0.04 ± 0.02, 19.9±0.1	15.56, 2.18	?	this work
ESO 499 G37$^{\circ,expo1}$	1.10 ± 0.10, 18.4±0.1	13.20, 17.52	N	this work
ESO 548 G10$^{\circ,expo2}$	0.07 ± 0.05, 19.5±0.4	17.60, 2.33	?	this work
ESO 548 G29$^{\circ,expo1}$	0.08 ± 0.03, 21.7±0.4	13.53, 12.13	Y	this work
NGC 488$^{R^{1/4}}$	> 19.5	10.2, 40.0	N	paper I
NGC 986$^{*,\circ,\odot}$	0.18 ± 0.05, 15.9±0.4		Y	NSBP
NGC 1345$^{\circ,expo1}$	0.08 ± 0.04, 21.0±0.3	13.67, 5.89	Y	this work
NGC 1483$^{\circ,expo1}$	< 0.04, 21.7±0.2	13.24, 13.33	Y	this work
NGC 1688$^{\circ,\odot}$	0.11 ± 0.05, 19.5±0.3 0.12 ± 0.02, 19.7±0.3		Y	NSBP
NGC 2104°	0.13 ± 0.05, 22.6±0.1		N	NSBP
NGC 2344$^{R^{1/4}+expo}$	> 19.5	13.39, 6.18	N	paper I
NGC 2460$^{*,R^{1/4}+expo}$	> 18.9	13.56, 3.93	N	paper I
NGC 2758$^{\circ,expo2}$	0.12 ± 0.05, 20.3±0.3	15.20, 2.81	?	this work
NGC 3259$^{\circ,expo2}$	< 0.04, 19.4±0.1	16.66, 1.13	N	this work
NGC 3898$^{R^{1/4}+expo}$	> 19.1	11.06, 11.74	?	paper I
NGC 3900$^{R^{1/4}+expo}$	> 18.5	13.50, 2.85	?	paper I
NGC 3928$^{\circ,\odot}$	0.10 ± 0.05, 17.0±0.3		N	NGF
NGC 4384$^{\circ,\odot}$	0.08 ± 0.03, 21.7±0.3		?	NGF
NGC 6340$^{R^{1/4}+expo}$	> 19.6	12.22, 8.03	N	paper I
NGC 7280$^{R^{1/4}+expo}$	> 18	12.84, 3.51	N	paper I

Table 3: Bulge and central compact source parameters for the galaxies of paper I (used in the present analysis). * indicates an inner morphology heavily influenced by dust obscuration. $^\circ$ indicates that the galaxy contains several bright sources in the nuclear region. $^\odot$ indicates nuclear star formation. ^{SFRNS} indicates a morphology similar to the star forming rings/arms in nuclear starbursts. † The column gives the FWHM (in $''$) and the apparent F606W magnitudes for the central compact sources. ‡ The column lists the total apparent magnitude in F606W and the half-light radius R_e (in $''$) of the spheroidal components identified by the analytical fits to the surface brightness profiles. Close to the galaxy name, the superscript $R^{1/4}$, $R^{1/4}$-*expo*, *expo1* or *expo2* identifies galaxies whose PC surface brightness distribution has been fitted with an $R^{1/4}$-law, an $R^{1/4}$-law plus exponential profile, a single- or double-exponential profile, respectively. Symbols in the column "Bar" are as in Table 2. For easy referencing, we identify in the last column the source for the analytical fits to the bulges, and include in the table also those galaxies which have no good fit ("NGF") or no surface brightness profile ("NSBP") , but host a central compact source used in the present analysis.